Int. Journ. of Laser Science, Vol. 1, pp. 123–133
Reprints available directly from the publisher
Photocopying permitted by license only

About a Photonic Crystal Nanocavity Based on a Nb_2O_5 Substrate

C-C. WEN* N. XU AND Y-G. FU

School of Opto-electronic Engineering, Changchun University of Science and Technology, Changchun 130022, Jilin Province, China

A description of developing a photonic crystal nanocavity is presented. The designing of a nanocavity on a Nb_2O_5 substrate was analysed by the finite difference time-domain (FDTD) method to find the resonant frequency, quality factor and mode profile of the cavity mode. The result showed that the resonant frequencies are 179 and 193 THz and by photoluminescence 190 to 250 THz. By optimizing the inner radius of the hole defects to achieve the best quality factor, the diameter was 0.170 μm and that of outside holes was 0.194 μm.

Keywords: Laser, photonic crystal, Nb_2O_5, nanocavity, finite difference time-domain (FDTD) method, resonant frequency, mode profile

1 INTRODUCTION

In 1987 Yablonovitch [1] and John [2] mentioned the concept of photonic crystal which showed that the material dielectric constant presents the sub-wavelength periodic characteristics in the spatial area. From the Maxwell's equations, light propagating through photonic crystal showed photonic band-gap effect, which demonstrate light must not spread through this structure if the frequency exactly lies in bandgap interval. The photonic crystal provide a novel performance of controlling photon which different from traditional method based on total internal reflection machine.

Until now many scientists have focused on research and design about two-dimensional photonic crystal, whilst three-dimensional (3-D) photonic crystals have been not been perfected due to fabrication technology limitations.

*Corresponding author: E-mail: fuyg@cust.edu.cn

2-D photonic crystals can be applied to optical communicating devices, low threshold microlasers, microsensors and cavity-quantum electrodynamics research [3, 4]. Photonic crystal nanocavity lasers have high quality factor, Q, and small mode volume, and theoretical mode properties can be achieved by proper cavity design [5]. Conventional types of microcavity have Fabry-Perot cavity, whispering gallery and photonic crystal dot defect nanocavity [6].

The developing direction of the nanocavity laser are mainly these two aspects: decreasing threshold current and increasing working temperature [7–9]; and improving microdisk laser coupling efficiency and achieving orientation output. Such application areas include vertical-cavity surface-emitting lasers (VSEL), microdisk/ring or regular polygon shape lasers emitting different wavelength laser light with various material [10].

In this paper the photonic crystal nanocavities were analysed by the finite difference time-domain method (FDTD) on Nb_2O_5 substrate for the first time to find the resonant frequency and mode profile of the cavity mode. We have optimized the inner radius of the defect dots holes to get best resonant frequency.

2 FINITE DIFFERENCE TIME-DOMAIN (FDTD) THEORY

Starting from Maxwell's equations:

$$\nabla \vec{E} = \frac{\rho}{\varepsilon_0} \tag{1}$$

$$\nabla \times \vec{E} = -\frac{\partial \vec{B}}{\partial t} - s\vec{H} \tag{2}$$

$$\nabla \vec{B} = 0 \tag{3}$$

$$\nabla \times \vec{H} = \vec{J} + \frac{\partial \vec{D}}{\partial t} \tag{4}$$

The coil curl equations can be derived to give six equations in three dimensions:

$$\frac{\partial H_x}{\partial t} = \frac{1}{\propto}\left(\frac{\partial E_y}{\partial z} - \frac{\partial E_Z}{\partial y} - sH_x\right) \tag{5}$$

$$\frac{\partial E_x}{\partial t} = \frac{1}{\varepsilon}\left(\frac{\partial H_z}{\partial y} - \frac{\partial H_y}{\partial z} - \sigma E_x\right) \tag{6}$$

$$\frac{\partial H_y}{\partial t} = \frac{1}{\propto}\left(\frac{\partial E_z}{\partial x} - \frac{\partial E_x}{\partial z} - sH_y\right) \tag{7}$$

$$\frac{\partial E_y}{\partial t} = \frac{1}{\varepsilon}\left(\frac{\partial H_x}{\partial z} - \frac{\partial H_z}{\partial x} - \sigma E_y\right) \tag{8}$$

$$\frac{\partial H_z}{\partial t} = \frac{1}{\propto}\left(\frac{\partial E_x}{\partial y} - \frac{\partial E_y}{\partial x} - sH_z\right) \tag{9}$$

$$\frac{\partial E_z}{\partial t} = \frac{1}{\varepsilon}\left(\frac{\partial H_y}{\partial x} - \frac{\partial H_x}{\partial y} - \sigma E_z\right) \tag{10}$$

In the Yee cell the function $F(x,y\,z)$ can be wrote into $F^n(i,j,k) = F(iDx,iDy,jDz)$. The second order degree of accuracy of core difference would be applied in space:

$$\frac{\partial F^n(i,j,k)}{\partial x} = \frac{F^n\left(i+\frac{1}{2},j,k\right) - F^n\left(i-\frac{1}{2},j,k\right)}{\Delta x} + o\left[(\Delta x)^2\right] \tag{11}$$

and in time:

$$\frac{\partial F^n(i,j,k)}{\partial t} = \frac{F^{n+\frac{1}{2}}(i,j,k) - F^{n-\frac{1}{2}}(i,j,k)}{\Delta t} + o\left[(\Delta t)^2\right] \tag{12}$$

Meanwhile more equations can be derived; for example:

$$E_x^{n+1}\left(i+\frac{1}{2},j,k\right) = \frac{1-\dfrac{\sigma\left(i+\frac{1}{2},j,k\right)\Delta t}{2\varepsilon\left(i+\frac{1}{2},j,k\right)}}{1+\dfrac{\sigma\left(i+\frac{1}{2},j,k\right)\Delta t}{2\varepsilon\left(i+\frac{1}{2},j,k\right)}} E_x^n\left(i+\frac{1}{2},j,k\right) + \frac{\Delta t}{\varepsilon\left(i+\frac{1}{2},j,k\right)} \cdot \frac{1}{1+\dfrac{\sigma\left(i+\frac{1}{2},j,k\right)\Delta t}{2\varepsilon\left(i+\frac{1}{2},j,k\right)}} \left[\frac{H_z^{n+\frac{1}{2}}\left(i+\frac{1}{2},j+\frac{1}{2},k\right) - H_z^{n+1/2}\left(i+\frac{1}{2},j-\frac{1}{2},k\right)}{\Delta y} + \frac{H_y^{n+\frac{1}{2}}\left(i+\frac{1}{2},j,k-\frac{1}{2}\right) - H_y^{n+1/2}\left(i+\frac{1}{2},j,k+\frac{1}{2}\right)}{\Delta z}\right] \tag{13}$$

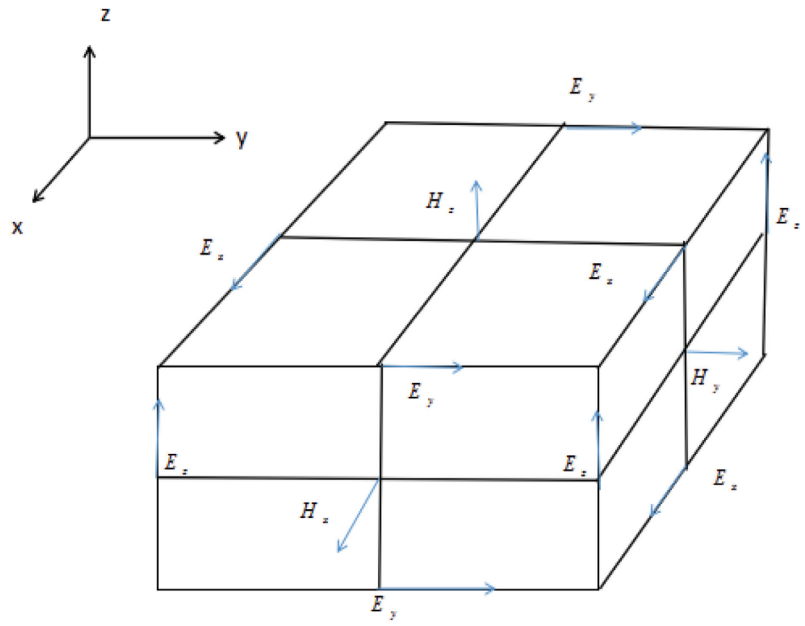

FIGURE 1
The discrete Yell cell in the FDTD.

where H is the magnetic field density, ρ is the charge density, σ is the electrical conductivity, E is the electrical field density, ε is the electric permittivity, J is the current density, B is the magnetic flux density, μ is the magnetic conductivity, D is the dielectric flux density and s is the magnetic loss. Figure 1 shows the Yee cell in the FDTD.

Perfect matched layer (PML) absorbing boundary conditions are usually applied in mathematical calculation and it has proven to be the most efficient technique. The key characteristic for PML that distinguish it from an ordinary layer is that wave incident on the PML from a non-PML medium cannot reflect at the interface. Due to the discrete Yell cell in FDTD and boundary conditions, the electric filed and magnetic field can be calculated in any space or time if only the size of Yell cell is small enough.

3 SIMULATION

The mathematic methods focusing on this aspect mainly includes FDTD, plane wave expansion, transferring matrix and scattering matrix. Meanwhile, the first method is more accurately and common in simulation but cost computational time. Firstly, simulation set up physical model on Nb_2O_5 substrate [11] with FDTD, and refraction index is 2.25. This kind of photonic crystal

was choose hexagonal lattice band structure and lattice constant is 0.575 μm and inner radius of holes is 0.194 μm initially. Next the dot defect cavity was added into the above band structure and the H number was Set 2. The picture of model is shown in Figure 2.

Figure 2 shows the top view and side view and graphic model of hexagonal photonic crystal array and nanocavity respectively. Then in these pictures the green arrow represent the magnetic dipoles and yellow block occupy effective simulation area. The property of direction of the *z*-axis was found to be symmetric and so the running time can be cut down to a half of that. Within the total simulation region, the *x*-span of effective area is 6.900 μm, *y*-span of that is 5.976 μm and *z*-span is 3.000 μm Boundary conditions along all directions were used with PML absorbing boundary conditions and *z*-min region was symmetric or antisymmetric boundary to decrease running time. Then the *x*-span of Yee cell [12] size was 0.072 μm, *y*-span of that was 0.062 μm. After finishing model construction, arrange for simulation process decide to arrange for proper environment. Experiment consider two magnetic dipoles as photoluminescence placed the middle of *z*-directional photonic crystal nanocavity. Its frequency bandwidth was from 160 to 250 THz. Last

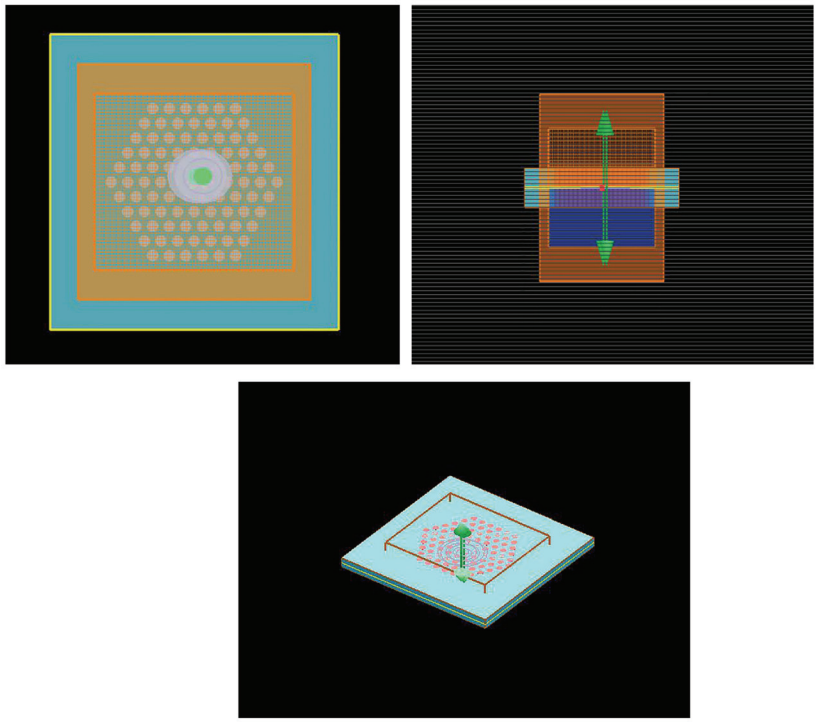

FIGURE 2
Model of a hexagonal photonic crystal nanocavity.

but not least, inserting quality factor analysis group to get the resonant frequency. Once experiment got resonant frequency, it can used mode profile monitor to record the mode properties of nanocavity. If the quality factor analysis group was placed where the light intensity is the strongest and the quality factor was calculated under this cavity structure parameters. Optimizing the inner radius of middle defect dot holes and searching for best quality factor

The fabrication of this structure are mostly involved with Micro/Nano manufacturing technology and what is suitable for visible or infrared laser output are like mask fabricating technology; for example, lithography, self-assembly and nanoimprinting. Or, by way of dry etching and wet etching, like reaction ion etch, ionic beam etch and inductively coupled plasma etching, etc. [13, 14].

4 RESULTS AND DISCUSSION

Importantly, the magnetic dipole could not be placed at the middle of the 3-D photonic crystal structure because it would decrease the opportunity to make a light source lie in the resonant nodes or mode zero point. At the current time the light energy was pumped into the simulation region and gradually decayed during simulation time. Before running simulations of these periodic structures, it was necessary and practical to use index monitors to check whether the structure was actually periodic when it was meshed into net lattice.

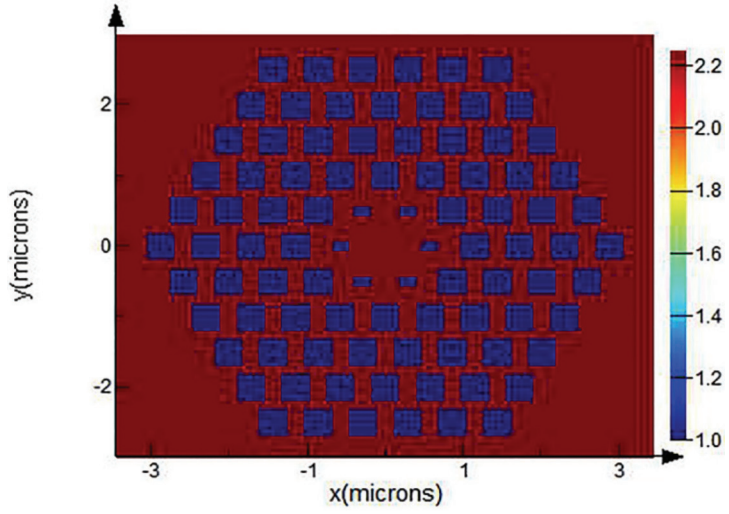

FIGURE 3
Refractive index of the photonic crystal nanocavity in simulation.

Refractive index checking results (see Figure 3) show that the holes were square shape. That was because the mesh maybe a little coarse. We characterized that each cross is identical and all array holes are uniform except for dot defect at the middle of this structure. Overall, it was essential to make sure that all the holes are meshed in the same way. Notably, it was not possible to view the meshed structure with the refractive index monitor in layout mode.

The, resonant frequencies of the cavity were calculated using time monitors to record the resonant fields as a function of time. Plotting the spectrum of the time monitor results, that was the Fourier transformed time signal, would produce peaks at some special resonant frequencies. It was then necessary to locate the locations of the peaks in resulted data array.

The results of the resonant frequency examination are shown in Figure 4 and it can be seen that the resonant frequency is about 179 and 193 THz when the magnetic dipole are given light with frequency from 190 to 250 THz. Comparatively, other resonant frequency could be chosen if necessary and the simulation algorithm would just change the parameters choosing special frequency filter from above spectrum.

In order to plot mode profiles of this nanostructure under light pumping we needed to isolate the mode of frequency of interest. Frequency domain power or profile monitor in FDTD provided the resulting mode profile plotting method. To isolate a mode of interest, it might need to use symmetry boundary conditions when modes of this structure produced. It ought to record the results at the resonant frequencies of the mode. In Figure 5,

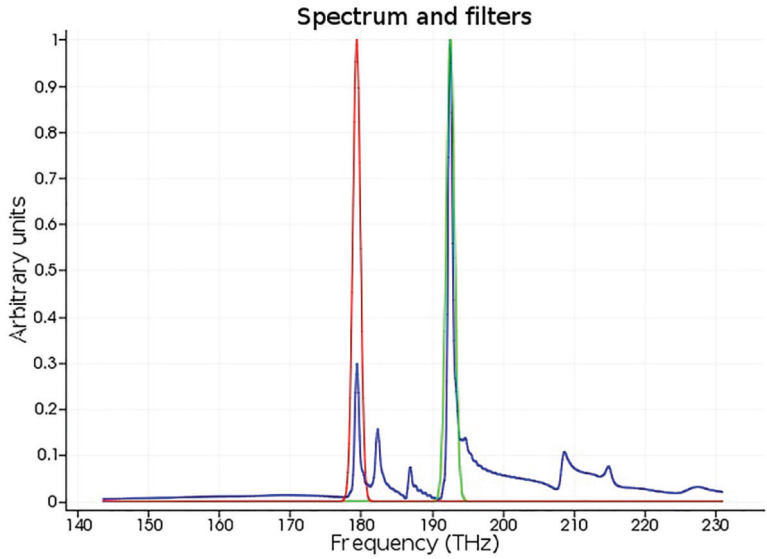

FIGURE 4
Plot showing the resonant frequency of the tested nanocavity.

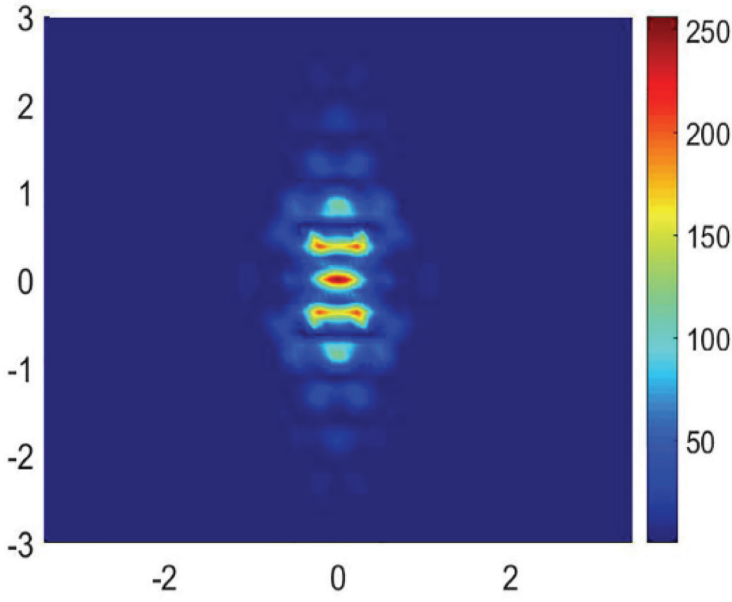

(a)

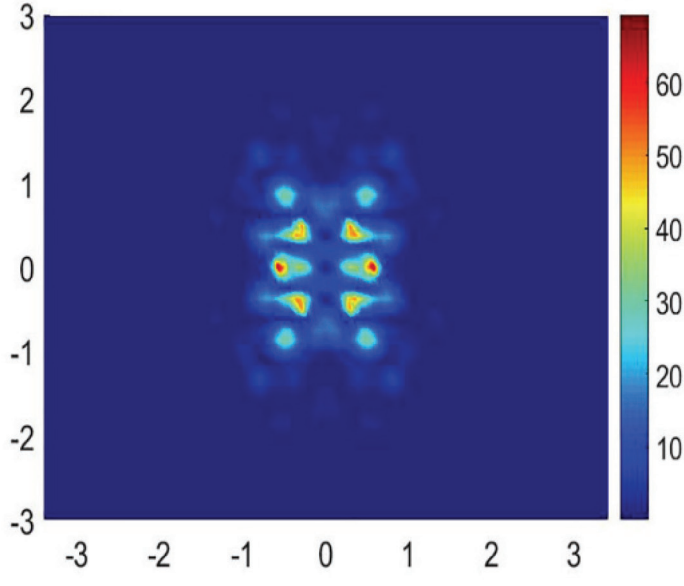

(b)

FIGURE 5
Mode profile under resonant frequency of (a) 179 THz and (b) 193 THz.

these two pictures provide evidence about the mode profile of two resonant frequencies, these are 179 and 193 THz. Through amplification of resonate frequency many times, studies serve as a proof that the output wavelength of laser radiation will be mainly approximately 1.550 μm.

After the resonant frequency was confirmed, the mode profile of each frequency can be described by power profile monitors, and the interesting frequency should be isolated certainly. Following pictures describe the details about distribution of mode profile of amplifying frequency. It is known that the physics quantity of *x*- and *y*-axis directions mean that the size of nanocavity in axis of coordinates and the length unit is micrometre. Results confirmed that these two distributions of mode are symmetric because of the structure characteristic of nanocavity. On the other hand, if boundary conditions are changed; for example, the *y*-min boundary conditions or *x*-min boundary conditions of the PML get into antisymmetric or symmetric, the mode profile would be more different than before.

The quality factor analysis group recorded the transmission as a function of frequency to calculate the quality factor at first. Next, it used

$$Q = \frac{f}{\Delta f} \tag{14}$$

to find out the quality factor from the transmission spectrum in results, where f is the resonant frequency and Δf is the full width at half maximum (FWHM). Then, calculating the envelope of the time-domain field signal accurately and next isolating each resonance peak in the frequency domain with a Gaussian filter, and taking the inverse Fourier transform to record the time decay separately for each peak. Meanwhile, the slope of the time decay function line was then used to calculate the quality factor and obtained an error estimate. Results found that quality factor of this nanocavity have certain relationship as a function of wavelength. Finally, computational process aimed at getting best quality factor will be operated and the optimized quality factor was calculated by adjust the inner radius of quantum dot holes most times. In practice, after this parameter being simply optimized by swarm particle optimization [14], the size is confirmed about 0.170 μm. Although there are important discoveries revealed by these studies, there are also limitations lacking of fabrication. Previous strategies offer a treatment to fabrication of photonic crystal nanocavity structure. Experiment will explore microfabrication and nanofabrication technologies for Nb_2O_5 especially, a key direction in the future.

5 CONCLUSIONS

The resonant frequency of a photonic crystal nanocavity on a Nb_2O_5 substrate was calculated by the finite difference time-domain (FDTD) method in the

first instance, yielding results are 179 and 193 THz, and then by photo luminescence of the light wavelength which gave 190 to 250 THz when inner radius of defect holes was 0.100 μm and the radius of periodic array holes was 0.194 μm. The mode profile of the resonant frequency was then plotted and analysed by a frequency power monitor. The quality factor was calculated and optimized by adjusting the inner radius of the middle defect holes of the periodic structure. The diameter of defect holes of about 0.170 μm and that of outside holes of 0.194 μm were determined to be optimum for achieving the best quality factor.

ACKNOWLEDGEMENTS

I would like to show my deepest gratitude to my supervisor, Prof. Fu, a respectable and responsible scholar. It is his support that has helped me complete this research work. I would also like to thank the Lumerical Company for its software knowledge, guidance and simulation experience which assisted the completion of this paper. Thanks too to the Natural Science Foundation of Jiangsu Province (No. 20150101038JC).

NOMENCLATURE

B	Magnetic flux density (Wb/m^2)
D	Dielectric flux density (C/m^2)
E	Electrical field density (V/m)
f	Resonant frequency (Hz)
Δf	Full width at half maximum (FWHM) (Hz)
H	Magnetic field density (T)
J	Current density (A/m^2)
s	Magnetic loss (T/cm)

Greek symbols

μ	Magnetic conductivity (H/m)
ρ	Charge density (C/m^2)
σ	Electrical conductivity (μS/cm)
ε	Electric permittivity (F/m)

REFERENCES

[1] Yablonovitch E. Inhibited spontaneous emission in solid-state physics and electronics. *Physical Review Letters* **58** (1987), 2059

[2] John S. Strong localization of photons in certain disordered dielectric superlattices. *Physical Review Letters* **58** (1987), 2486–2489.

[3] Kong X-L. Negative Refractive Index Phenomenon in Photonic Crystal and Mode Properties of Anisotropic Optical Circular Microcavity Analysis. PhD Thesis, University of Science and Technology of China. 2010.

[4] Joo X-S. Novel Silica Optical Microcavities and Applications. PhD Thesis, Zhejiang University. 2010.

[5] Lee P.T., Lu T.W. and Fan J.H. High quality factor microcavity lasers realized by circular photonic crystal with isotropic photonic band gap effect. *Applied Physics Letters* **90**(15) (2007), 151125.

[6] Wong W-G. Research on mode properties of hexagonal micro-cavity lasers. MSc Dissertation, Huaqiao University .2010

[7] Takiguchi M., Taniyama H. and Sumikura H. Systematic study of thresholdless oscillation in high-β buried multiple-quantum-well photonic crystal nanocavity lasers. *Optics Express* **24**(4) (2016), 3441–3450.

[8] Xue W., Yu Y. and Ottaviano L. Threshold characteristics of slow-light photonic crystal lasers. *Physical Review Letters* **116**(6) (2016), 063901.

[9] Jagsch S.T., Triviño N.V., Lohof F., Callsen G., Kalinowski S., Rousseau I.M., Barzel R., Carlin J-F., Jahnke F., Butté R., Gies C., Hoffmann A., Grandjean N. and Reitzenstein S. Thresholdless lasing of nitride nanobeam cavities. *The 25th International Semiconductor Laser Conference (ISLC2016)*. 12–15 September 2016, Kobe, Japan.

[10] Miyazono E., Zhong T. and Craiciu I. Coupling of erbium dopants to yttrium orthosilicate photonic crystal cavities for on-chip optical quantum memories. *Applied Physics Letters* **108**(1) (2016), 011111.

[11] Tang Y., Merz J.L., Tokranov V. and Oktyabrsky S. Characterization of 2D-photonic crystal nanocavities by polarization-dependent photoluminescence. *Proceedings of 2005 5th IEEE Conference on Nanotechnology, 2005*. 15 July 2005, Nagoya, Japan. pp. 35–38

[12] Hagness S.C. FDTD Computational Electromagnetics Modeling of Microcavity Lasers and Resonant Optical Structures. PhD Thesis, Northwestern University, 1998.

[13] Serafimovich P.G., Stepikhova M.V. and Kazanskiy N.L. On a silicon based photonic-crystal cavity for the near-IR region: Numerical simulation and formation technology. *Semiconductors* **50**(8) (2016), 1112–1116.

[14] Robinson J. and Rahmat-Samii Y. Particle swarm optimization in electromagnetics. *IEEE Transactions on Antennas and Propagation* **52** (2004), 397–407